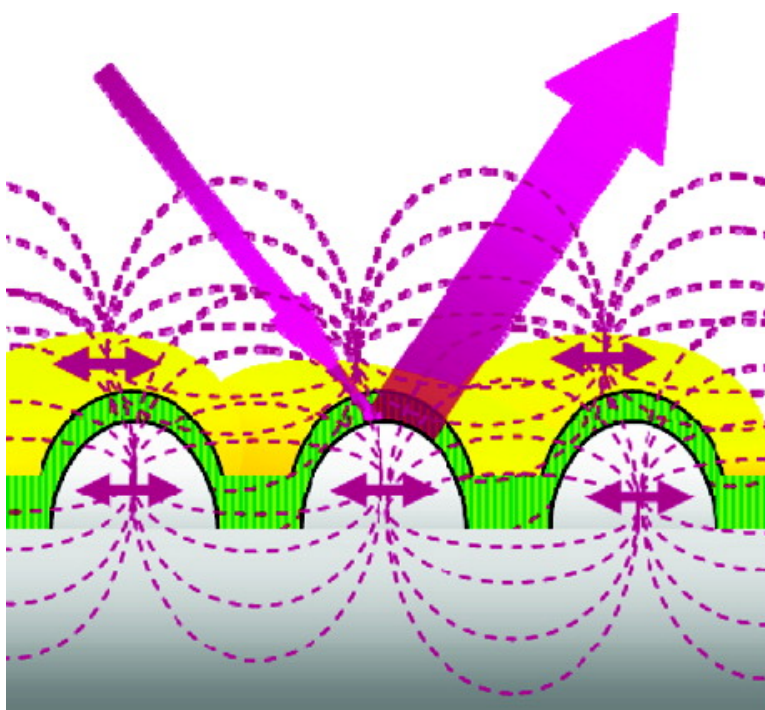


## Novel Au#Ag Hybrid Device for Electrochemical SE(R)R Spectroscopy in a Wide Potential and Spectral Range

Jiu-Ju Feng, Ulrich Gernert, Murat Sezer, Uwe Kuhlmann, Daniel H. Murgida, Christin David, Marten Richter, Andreas Knorr, Peter Hildebrandt, and Inez M. Weidinger

*Nano Lett.*, **2009**, 9 (1), 298-303 • DOI: 10.1021/nl802934u • Publication Date (Web): 22 December 2008

Downloaded from <http://pubs.acs.org> on January 23, 2009



### More About This Article

Additional resources and features associated with this article are available within the HTML version:

- Supporting Information
- Access to high resolution figures
- Links to articles and content related to this article
- Copyright permission to reproduce figures and/or text from this article



# NANO LETTERS

Subscriber access provided by UNIV NAC DE BUENOS AIRES

[View the Full Text HTML](#)



**ACS Publications**  
High quality. High impact.

Nano Letters is published by the American Chemical Society, 1155 Sixteenth Street N.W., Washington, DC 20036

# Novel Au–Ag Hybrid Device for Electrochemical SE(R)R Spectroscopy in a Wide Potential and Spectral Range

Jiu-Ju Feng,<sup>†</sup> Ulrich Gernert,<sup>‡</sup> Murat Sezer,<sup>†</sup> Uwe Kuhlmann,<sup>†</sup> Daniel H. Murgida,<sup>||</sup> Christin David,<sup>§</sup> Marten Richter,<sup>§</sup> Andreas Knorr,<sup>§</sup> Peter Hildebrandt,<sup>†</sup> and Inez M. Weidinger<sup>\*†</sup>

*Institut für Chemie, Technische Universität Berlin, Sekr. PC 14, Strasse des 17, Juni 135, D-10623 Berlin, Germany, Zentraleinrichtung Elektronenmikroskopie, Technische Universität Berlin, Strasse des 17, Juni 135, D 10623 Berlin, Germany, Institut für Theoretische Physik, Technische Universität Berlin, EW 7-1, Hardenbergstr.36, D-10623 Berlin, Germany, and Departamento de Química Inorgánica, Analítica y Química Física/INQUIMAE, Universidad de Buenos Aires, Ciudad Universitaria, Pab. 2, piso 1, C1428EHA Buenos Aires, Argentina*

Received September 26, 2008; Revised Manuscript Received December 2, 2008

## ABSTRACT

A nanostructured gold–silver-hybrid electrode for SER spectroelectrochemistry was developed which advantageously combines the electrochemical properties and chemical stability of Au and the strong surface enhancement of (resonance) Raman scattering by Ag. The layered device consists of a massive nanoscopically rough Ag electrode, a thin (2 nm) organic layer, and a ca. 20 nm thick Au film that may be coated by self-assembled monolayers for protein adsorption. The SERR-spectroscopic and electrochemical performance of this device is demonstrated using the heme protein cytochrome c as a benchmark model system, thereby extending, for the first time, SE(R)R studies of molecules on Au surfaces to excitation in the violet spectral range. The enhancement factor is only slightly lower than for Ag electrodes which can be rationalized in terms of an efficient transfer of plasmon resonance excitation from the Ag to the Au coating. This mechanism, which requires a thin dielectric layer between the two metals, is supported by theoretical calculations.

Surface enhanced Raman (SER) spectroscopy is a well-established technique in various fields of (bio)analytical chemistry and interfacial sciences.<sup>1–6</sup> The method exploits the enhancement of the Raman scattering from molecules in the proximity of nanoscopically rough metal surfaces due to the coupling of the oscillating electric field of the incident and scattered radiation with the surface plasmons of the metal. Of special interest is the combination of SER spectroscopy with electrochemical methods for applications in bioelectrochemistry or biosensors. Such a SER-active device can be constructed using electrochemically roughened electrodes or thin films, which are adsorbed via electrodeposition on a structured template.

The enhancement of SER-active electrodes is primarily determined by the wavelength-depending dielectric properties of the metal that largely restrict the applicability of SER

spectroscopy to Ag and Au. Whereas Ag provides a good enhancement throughout the visible and near-infrared region, Au is applicable for SER spectroscopy only for excitation wavelengths above ca. 550 nm since below this wavelength photoinduced transitions from d-band electrons to the conducting band effectively damp the surface plasmon resonances.

However, for SER spectroscopy, excitation below 550 nm is preferable since, according to the  $\nu^4$ -law, the intrinsic Raman intensity increases with decreasing excitation wavelength. Furthermore, the vast majority of molecules exhibit electronic transitions below 550 nm such that the combination of the molecular (pre)resonance Raman and the SER effect (surface enhanced resonance Raman, SERR), which drastically increases the sensitivity, can mainly be exploited with excitation wavelengths shorter than 550 nm. Thus, a significantly higher sensitivity of SE(R)R measurements is usually achieved with Ag surfaces. On the other hand, using Ag as a substrate is associated with a serious drawback specifically for spectroelectrochemical and biological applications. First, due to the low oxidation potential, SER-

\* To whom correspondence should be addressed. E-mail: i.weidinger@mailbox.tu-berlin.de.

<sup>†</sup> Institut für Chemie, Technische Universität Berlin.

<sup>‡</sup> Zentraleinrichtung Elektronenmikroskopie, Technische Universität Berlin.

<sup>§</sup> Institut für Theoretische Physik, Technische Universität Berlin.

<sup>||</sup> Universidad de Buenos Aires.

spectroscopic studies with Ag electrodes are limited to a distinctly narrower potential range than with Au electrodes. Second, Au is a more biocompatible metal than Ag that, in contact with aqueous solutions, inevitably forms  $\text{Ag}^+$  cations that can attack and degrade biopolymers. For these reasons, it would be highly desirable to fabricate SER-active Au-based substrates with surface plasmon resonances at higher energies such that the specific advantages of Au and Ag can be combined.

Considerable efforts have been made to design Au–Ag hybrid systems, such as mixed Ag(core)/Au(shell) nanoparticles<sup>7–11</sup> or Ag(Au) nanoparticles immobilized on metal supports.<sup>12–14</sup> Although the Ag–Au interactions caused changes of the surface plasmon resonances of the hybrid systems none of these systems reported so far have led to a surface enhancement of the Raman scattering for adsorbates below 500 nm.

In the present work, we have employed a different strategy to construct an Au–Ag hybrid device in which both metals are separated by an ultrathin insulating organic film. This device exhibits the electrochemical properties of an Au electrode while the optical properties are very similar to that of Ag surfaces. The performance of the Au–Ag hybrid electrode is tested by using the heme protein cytochrome *c* (Cyt-*c*) as a benchmark system for biological applications. Cyt-*c* has been characterized in numerous studies by cyclic voltammetry (CV) and SERR spectroscopy when immobilized on Au and Ag electrodes, respectively.<sup>1,15–20</sup> The protein can be electrostatically bound to Au and Ag electrodes coated with self-assembled monolayers (SAMs) of carboxyl-terminated mercaptanes revealing an ideal Nernstian behavior. Because of the strong electronic transition of the heme group at ca. 410 nm, excitation at 413 nm affords intense SERR spectra of the cofactor solely of the immobilized proteins on Ag surfaces.<sup>17,21</sup>

In the present approach, a Ag electrode, mechanically polished and electrochemically roughened as described previously,<sup>22</sup> served as support for the hybrid system. The surface morphology of the roughened Ag electrode was characterized by scanning electron microscopy (SEM) revealing a porous surface structure with a grain size between 60 and 100 nm (Figure 1A).

The electrode was subsequently immersed in a 1 mM 11-amino-1-undecanethiol (AUT) solution in ethanol for 24 h to form stable self-assembled monolayers (SAMs). After gently washing with ethanol, the SAM-modified electrode was treated with a 1% (wt)  $\text{AuCl}_4^-$  solution in ethanol for 2–4 h and subsequently rinsed with ethanol and dried under nitrogen. Finally, the electrode was inserted into a deaerated 0.1 M KCl solution to reduce the adsorbed  $\text{AuCl}_4^-$  ions at  $-0.5$  V (versus 3 M Ag/AgCl) for 5 min. To guarantee reproducible Au coverage, the reduction of Au(III) was monitored chronoamperometrically. Optimum SERRS intensity was found when the reductive current dropped to 1% of its initial value after ca. 30 s (See Figure 3B and Supporting Information). This characteristic reduction time  $\tau_{R(1\%)}$  depends on the incubation time of the Ag–AUT electrode in the  $\text{AuCl}_4^-$  solution, which was adjusted to

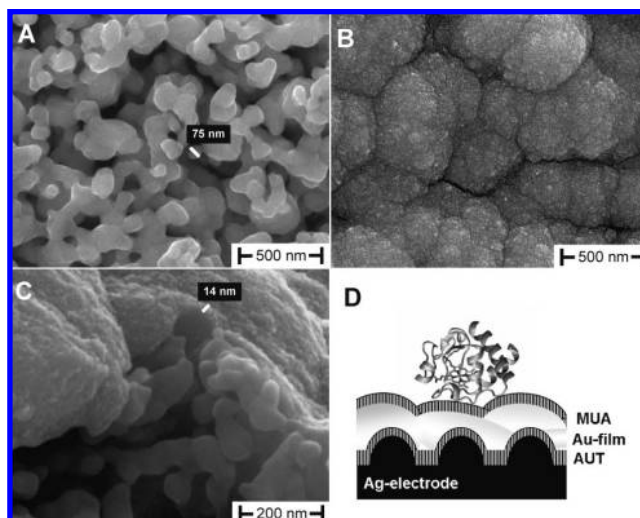


**Figure 1.** SEM images of SER-active Ag and Au–Ag hybrid electrodes. (A) Ag, top view, (B) Au–Ag, top view, and (C) Au–Ag, scratch through the layer. (D) Schematic illustration of Cyt-*c* adsorbed on the Au–Ag hybrid electrode.

achieve  $\tau_{R(1\%)} \approx 30$  s for all electrodes used in this work. SEM microscopic images demonstrate that Au islands are formed with an average lateral dimension of 300–400 nm and a thickness of less than 20 nm (Figure 1B,C). The SEM data further show a nearly complete coverage of the surface by the Au island films revealing a distinctly smoother and more homogeneous morphology than the Ag support (Figure 1A). Elementary analysis of the surface was performed with energy dispersive X-ray spectroscopy (EDX) confirming that the outer layer of the hybrid electrode consists of pure Au (Figure 2A). In Figure 2A, a representative EDX spectrum of the hybrid electrode (red) is compared with that of a reference system in which a massive smooth Ag electrode was sputtered with Au to form a 20 nm thick and uniform Au layer (blue). In both spectra, the intensity ratio of the Au and Ag peaks is the same which points to a similar Au layer thickness. Taking into account the dependence of the EDX intensity on the incident angle of the electron beam these results, therefore indicate that the Au layer thickness of the hybrid electrode is equal or less than 20 nm, which is consistent with the SEM data (vide supra).

For biocompatible immobilization of Cyt-*c* (yeast iso-1 cytochrome *c*), the Au surface of the Au–Ag hybrid device was coated with a mixed SAM of 11-mercapto-undecanoic acid (MUA) and 11-mercapto-1-undecanol (MU) by incubation in an equimolar (1 mM) ethanolic solution of MUA and MU for 24 h. Afterward the Au–Ag electrode was placed in an electrochemical cell using Pt wire as the counter electrode and Ag/AgCl (3 M KCl) as reference electrode. Electrostatic adsorption of the protein was achieved within 30 min at a potential of  $-0.4$  V from a diluted aqueous solution of Cyt-*c* (0.2–0.4  $\mu\text{M}$ ) buffered at pH 7.0.

The CV of Cyt-*c* adsorbed on the coated Au–Ag electrode was measured in a deaerated aqueous solution (pH 7.0) including 12.5 mM phosphate buffer and 12.5 mM potassium sulfate (Figure 2B). The CV displays nearly symmetric oxidative and reductive peaks indicating a reversible redox

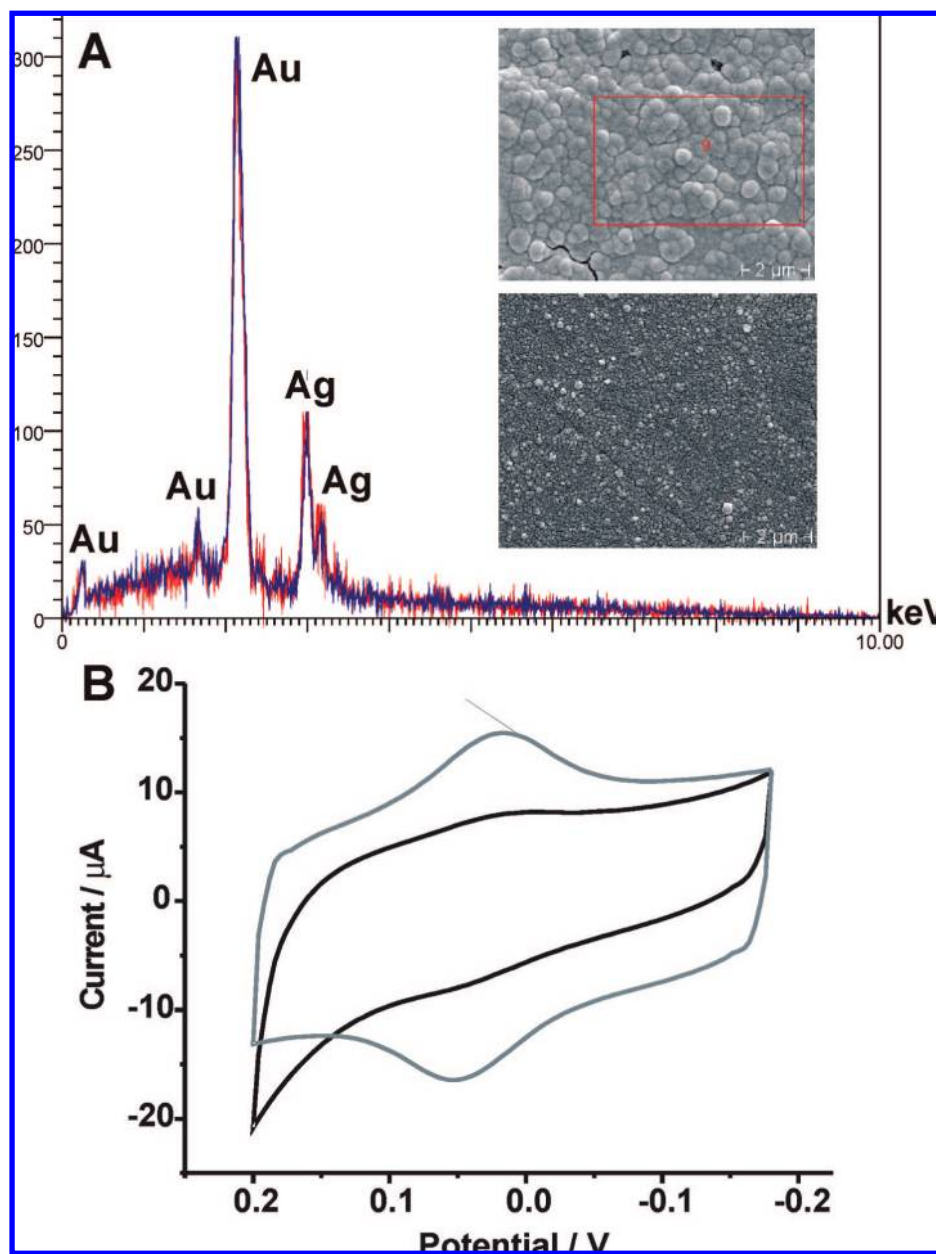


**Figure 2.** (A) EDX spectra of the Ag–Au electrode (red), determined from a spot of  $25 \mu\text{m}^2$ , and a smooth Ag reference system coated with a 20 nm Au film (blue). (Inset) SEM images of the samples used for EDX measurements (top, Au–Ag electrode; bottom, reference system) (B) Cyclic voltammograms of Cyt- c adsorbed on Ag (black) and Au–Ag (gray) electrodes coated with MUA/MU-SAMs (scan rate: 0.1 V/s).

reaction of the immobilized Cyt- c and a good electronic communication between the protein and the metal substrate. Integration of the peaks allows estimating the surface coverage of Cyt- c to be ca.  $8.5 \times 10^{-11} \text{ mol cm}^{-2}$ . The CV peaks are distinctly stronger than those in the CV obtained from Cyt- c immobilized on SAM-coated Ag electrodes, where a surface coverage of  $2.3 \times 10^{-11} \text{ mol cm}^{-2}$  was estimated. Furthermore, CV curves of Cyt- c on Au–Ag hybrid electrodes lack the oxidative peak of Ag at ca. +0.15 V. This finding implies that the electrochemical properties of the Au–Ag hybrid device are essentially the same as those of a pure Au electrode. It further confirms the conclusion drawn from the SEM and EDX measurements that Ag is not in contact with the aqueous solution.

SERR spectra of Cyt- c immobilized on SAM-coated Ag and Au–Ag hybrid electrodes were measured with 413 nm excitation using the experimental setup described previously.<sup>22</sup> SER activity on a rough metal surface decreases with time and preparation of the SAM-coated Ag and Au–Ag hybrid devices required 24 and 48 h, respectively. Thus, the comparison of the SERR spectra from both devices was made 48 h after roughening of the supporting metal. In all cases, the electrode potential was set to  $-0.4 \text{ V}$  such that the immobilized protein is fully reduced. Band positions and relative intensities of both SERR spectra are identical and also agree very well with the RR spectrum of Cyt- c in solution indicating that the native active structure is preserved upon immobilization on coated Ag and Au–Ag electrodes

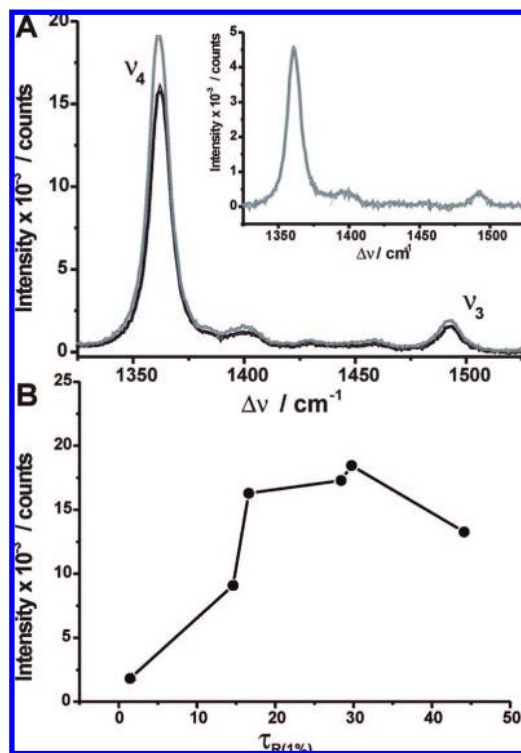


**Figure 3.** (A) SERR spectra of Cyt-c adsorbed on Ag (black) and Ag–AUT–Au (gray) electrodes. (Inset) SERR spectrum of Cyt-c adsorbed on Au–Ag electrodes with Au directly deposited on Ag without a dielectric spacer. The spectra were obtained with 413 nm excitation (2.5 mW) and 3 s accumulation time at an electrode potential of  $-0.4$  V vs Ag/AgCl. (B) SERR intensity of the  $\nu_4$  band ( $1360\text{ cm}^{-1}$ ) as a function of reduction time  $\tau_{R(1\%)}$  (see also Supporting Information).

(Figure 3A). As shown in Figure 3A, both types of electrodes provide nearly the same SERR intensities of the immobilized Cyt-c. If one corrects for the different Cyt-c surface coverage, the actual surface enhancement of Au–Ag electrodes is only ca. 4 times lower than that for Ag electrodes.

To explore the origin of the unexpected enhancement effect, various control measurements were carried out. First, no SERR signal could be detected from an AUT-coated Ag electrode in contact with a Cyt-c-containing solution. Thus, it can be ruled out that the SERR spectrum of Cyt-c on Au–Ag hybrid electrodes partially results from proteins that, due to holes in the Au island films, have been directly adsorbed on the AUT-coated Ag support. Second, using a mechanically polished and thus smoother Ag support affords a much weaker SERR spectrum of Cyt-c adsorbed on the coated Au overlay. Third, no SERR spectrum of Cyt-c was obtained with 413 nm excitation for Au–Au devices in which the Ag support is replaced by Au. Consequently, we conclude that optimum enhancement requires a nanoscopically rough Ag support for initial optical excitation in the violet region. In fact, due to interband electronic transitions, optical excitation of surface plasmon resonances of Au can be ruled out at 413 nm. Optical excitation of the underlying Ag support requires that the Au film is sufficiently transparent for the incident radiation (413 nm). This is indeed the case,

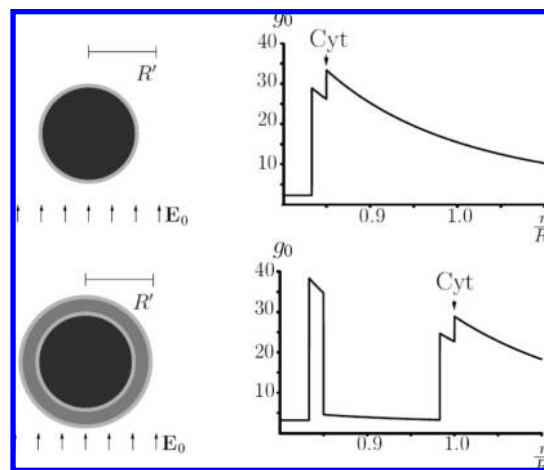


**Figure 4.** Distance-dependent electric field enhancement  $g_0$  calculated for a SAM-coated Ag sphere (top) and a SAM-coated Ag–SAM–Au sphere (bottom). The positions of the adsorbed Cyt-c are indicated by “Cyt”.

since according to the Fresnel theory for normal incidence, 44% of the incoming light is transmitted through a 16 nm gold film.

Direct deposition of Au island films on an electrochemically roughened Ag electrode affords a 4 times lower SERR signal as compared to hybrid devices including the dielectric spacing (Figure 3 A, inset). A comparable decrease in intensity was observed when a conductive (poly)ethyleneimine (PEI)/electrolyte layer is used as a spacer instead of AUT. We, therefore, conclude that an insulating thin film is required for optimum surface enhancement via the Au surface. This finding is supported by previously published theoretical and experimental results that indicate an increased surface enhancement for closely spaced but separated nanoparticles or films<sup>23–25</sup> as compared to nanostructured metal substrates.<sup>26</sup>

To rationalize the experimental findings, we have calculated the distance-dependent electric field enhancement for coated Ag and Au–Ag nanoparticles that may be considered as a first approximation for the nanoscopically rough surfaces of Ag and Au–Ag hybrid electrodes. The underlying model is based on an Ag sphere of 100 nm radius coated with a dielectric (SAM) layer of 2 nm thickness (Figure 4). The Au–Ag hybrid device is mimicked by adding a 16 nm thick Au shell and an additional SAM layer (2 nm). In both cases, water was used as surrounding medium. The dielectric functions for Ag and Au were taken from Johnson and Christy.<sup>27</sup> The permittivity of the SAM and H<sub>2</sub>O was assumed to be 2 and 1.77, respectively. Because of the size of the system the Maxwell equations were solved in the quasistatic approximation neglecting retardation effects. An expansion of the electrostatic potential in spherical harmonics was used to solve the Poisson equation in spherical coordinates where boundary conditions at the interfaces of the shells had to be matched. Because of the symmetry, only dipole modes contribute to the field enhancement defined by the square of the ratio of the electric field strengths in the presence and in the absence of the nanosphere (see Supporting Information for further details). The calculations refer to the field

enhancement of the incident radiation  $g_0$  at  $\nu_0 = 23\,420\text{ cm}^{-1}$ , which coincides with the plasmon resonance of the Ag sphere. The field enhancement of the Raman scattered radiation  $g_{\text{Ra}}$  (at  $\nu_{\text{Ra}}$ ) is not explicitly considered. In view of the underlying simplifications of the model, it is justified to assume  $g_0 \approx g_{\text{Ra}}$  such that the SER enhancement factor may be taken as  $|g_0|^2$ .<sup>28,29</sup> Then the magnitude of the enhancement factor is comparable to the one previously determined by Kerker et al. for Ag spheres of similar size.<sup>28</sup>

In Figure 4,  $g_0$  is plotted as function of  $r/R'$  where  $r$  is the distance from the center of the Ag sphere and  $R'$  represents the radius of the Au–Ag multilayer shell. For the Au–Ag particle at the SAM/water interface ( $r/R' = 1.0$ ) the field enhancement  $g_0$  is only slightly lower compared to the SAM/water interface of the Ag sphere ( $r/R' = 0.85$ ), which is in qualitative agreement with the experimental finding. Comparing the calculated data for  $r/R' = 1.0$ , the predicted field enhancement is nearly two times higher for Au–Ag than for Ag nanospheres. Again, these data are consistent with the experimental findings that in this wavelength region the inner AUT-SAM layer is essential for an efficient transfer of optical plasmon excitation from the Ag sphere to the Au coating.

The calculated field enhancement reveals a strong dependence on the permittivity of the media as indicated by the abrupt changes of  $g_0$  at the SAM/H<sub>2</sub>O interfaces (Figure 4). These breaks can be attributed to internal reflections at the interface between media of higher (SAM) and lower (H<sub>2</sub>O) permittivity. It is interesting to note that despite the attenuation of the incident light by the Au layer, a stronger electric field enhancement is predicted in the region of the AUT–SAM of the Ag/SAM/Au multilayer sphere as compared to the AUT-coated Ag nanoparticle. This result is in line with previous studies suggesting particular high field enhancements in the interspace between two metal particles.<sup>13,23,26</sup> Conversely, the lack of such a dielectric spacer between the metal layers may thus account for the attenuated SER intensities observed upon direct deposition of Au on Ag electrodes. An even stronger reduction of SER intensity for Au nanoparticles directly coated with SERS-inactive metals (Pt, Pd, or Ni) was found by Tian et al.<sup>30</sup> In the latter study, using 632 nm irradiation that provided optical excitation of the Au surface plasmons, a decrease of the enhancement by a factor of 10 was estimated for molecules adsorbed on the 7 nm thick layer of the inert metals.

The sensitivity of the Au–Ag hybrid device developed in this work is not restricted to excitation in the violet region. Upon 514 and 568 nm excitation, high quality SER spectra of Cyt-c adsorbed on Au–Ag-hybrid electrodes could be obtained with intensities comparable to those at pure Ag substrates (Figure 5). Furthermore, upon 647 nm excitation SER spectra of the MUA-SAM are weaker only by a factor of 2 on Au–Ag electrodes compared to Ag electrodes. These wavelength-dependent changes of the relative SE(R)R enhancement for Au–Ag hybrid and pure Ag electrodes can be understood in terms to the wavelength-dependent transmittance of the Au film, which for a thickness of 16 nm is calculated to be 77, 69, and 48% at 514, 568, and 647 nm, respectively.

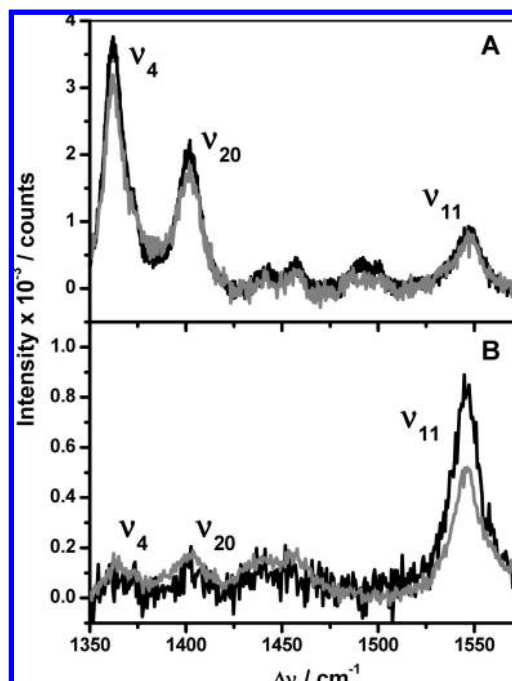


**Figure 5.** SERR spectra of Cyt-c on Ag (black) and Au–Ag (gray) electrodes at  $-0.4\text{ V}$  (vs Ag/AgCl) obtained upon excitation with (A) 514 nm (3.2 mW) and (B) 568 nm (1.5 mW). The accumulation time was 5 and 30 s for 514 and 568 nm excitation, respectively.

In summary, we have demonstrated that the novel Au–Ag hybrid device developed in this work is suitable for SE(R)R spectroscopy in the entire visible spectral region. Because of an efficient transfer of plasmon excitation from the Ag to the Au coating, the magnitude of the enhancement is comparable to that for pure Ag systems while displaying the electrochemical stability of gold. These properties expand the perspectives of applying SER-spectroscopic techniques, due to the better biocompatibility of Au and its significantly higher importance in heterogeneous catalysis as compared to Ag. These applications may include more sensitive approaches in detecting and identifying biomolecules in analytic assays by combining the molecular (pre)resonance and surface enhancement effects upon excitation in the violet region. This improved sensitivity of the hybrid devices may also allow for monitoring catalytic processes in situ with and without electrochemical control. Finally, these SER spectroscopic applications are not restricted to stationary measurements but may also be extended to the time-resolved domain to probe the dynamics of interfacial reactions, as already established for Ag electrodes.<sup>1</sup>

**Acknowledgment.** Financial support by the Fonds der Chemischen Industrie and the DFG (Cluster of Excellence UniCat and Sfb 448) is gratefully acknowledged.

**Supporting Information Available:** Chronoamperometric data on the preparation of hybrid electrodes and a brief outline of the theoretical concept of the field enhancement calculations. This material is available free of charge via the Internet at <http://pubs.acs.org>.

## References

- (1) Murgida, D. H.; Hildebrandt, P. *Chem. Soc. Rev.* **2008**, *37*, 937–945.
- (2) Moore, B. D.; Stevenson, L.; Watt, A.; Flitsch, S.; Turner, N. J.; Cassidy, C.; Graham, D. *Nat. Biotechnol.* **2004**, *22*, 1133–1138.
- (3) Graham, D.; Mallinder, B. J.; Whitcombe, D.; Watson, N. D.; Smith, W. E. *Anal. Chem.* **2002**, *74*, 1069–1074.
- (4) Shafer-Peltier, K. E.; Haynes, C. L.; Glucksberg, M. R.; Van Duyne, R. P. *J. Am. Chem. Soc.* **2003**, *125*, 588–593.
- (5) Zhang, X. Y.; Young, M. A.; Lyandres, O.; Van Duyne, R. P. *J. Am. Chem. Soc.* **2005**, *127*, 4484–4489.
- (6) Hering, K.; Cialla, D.; Ackermann, K.; Dorfer, T.; Moller, R.; Schneidewind, H.; Mattheis, R.; Fritzsche, W.; Rosch, P.; Popp, J. *Anal. Bioanal. Chem.* **2008**, *390*, 113–124.
- (7) Mulvaney, P.; Giersig, M.; Henglein, A. *J. Phys. Chem.* **1993**, *97*, 7061–7064.
- (8) Pande, S.; Ghosh, S. K.; Prahraj, S.; Panigrahi, S.; Basu, S.; Jana, S.; Pal, A.; Tsukuda, T.; Pal, T. *J. Phys. Chem. C* **2007**, *111*, 10806–10813.
- (9) Rivas, L.; Sanchez-Cortes, S.; Garcia-Ramos, J. V.; Morcillo, G. *Langmuir* **2000**, *16*, 9722–9728.
- (10) Kumar, G. V. P.; Shruthi, S.; Vibha, B.; Reddy, B. A. A.; Kundu, T. K.; Narayana, C. *J. Phys. Chem. C* **2007**, *111*, 4388–4392.
- (11) Hodak, J. H.; Henglein, A.; Giersig, M.; Hartland, G. V. *J. Phys. Chem. B* **2000**, *104*, 11708–11718.
- (12) Driskell, J. D.; Lipert, R. J.; Porter, M. D. *J. Phys. Chem. B* **2006**, *110*, 17444–17451.
- (13) Keating, C. D.; Kovaleski, K. K.; Natan, M. J. *J. Phys. Chem. B* **1998**, *102*, 9414–9425.
- (14) Kim, K.; Yoon, J. K. *J. Phys. Chem. B* **2005**, *109*, 20731–20736.
- (15) Nahir, T. M.; Clark, R. A.; Bowden, E. F. *Anal. Chem.* **1994**, *66*, 2595–2598.
- (16) Armstrong, F. A.; Wilson, G. S. *Electrochim. Acta* **2000**, *45*, 2623–2645.
- (17) Murgida, D. H.; Hildebrandt, P. *Phys. Chem. Chem. Phys.* **2005**, *7*, 3773–3784.
- (18) El Kasmi, A.; Wallace, J. M.; Bowden, E. F.; Binet, S. M.; Linderman, R. J. *J. Am. Chem. Soc.* **1998**, *120*, 225–226.
- (19) Xu, J. S.; Bowden, E. F. *J. Am. Chem. Soc.* **2006**, *128*, 6813–6822.
- (20) Millo, D.; Ranieri, A.; Koot, W.; Gooijer, C.; van der Zwan, G. *Anal. Chem.* **2006**, *78*, 5622–5625.
- (21) Murgida, D. H.; Hildebrandt, P. *Acc. Chem. Res.* **2004**, *37*, 854–861.
- (22) Wackerbarth, H.; Klar, U.; Günther, W.; Hildebrandt, P. *Appl. Spectrosc.* **1999**, *53*, 283–291.
- (23) Genov, D. A.; Sarychev, A. K.; Shalaev, V. M.; Wei, A. *Nano Lett.* **2004**, *4*, 153–158.
- (24) He, L.; Smith, E. A.; Natan, M. J.; Keating, C. D. *J. Phys. Chem. B* **2004**, *108*, 10973–10980.
- (25) Li, H. G.; Baum, C. E.; Sun, J.; Cullum, B. M. *Appl. Spectrosc.* **2006**, *60*, 1377–1385.
- (26) GarciaVidal, F. J.; Pendry, J. B. *Phys. Rev. Lett.* **1996**, *77*, 1163–1166.
- (27) Johnson, P. B.; Christy, R. W. *Phys. Rev. B* **1972**, *6*, 4370–4379.
- (28) Kerker, M.; Wang, D. S.; Chew, H. *Appl. Opt.* **1980**, *19*, 3373–3388.
- (29) Kerker, M. *Acc. Chem. Res.* **1984**, *17*, 271–277.
- (30) Tian, Z. Q.; Ren, B.; Li, J. F.; Yang, Z. L. *Chem. Commun.* **2007**, 3514–3534.

NL802934U